Synthesis, Characterization, and Adsorbate Interactions of CoAPO-41 and CoAPSO-41 Molecular Sieves

A. M. Prakash,[†] Martin Hartmann,[‡] and Larry Kevan*[,†]

Department of Chemistry, University of Houston, Houston, Texas 77204-5641, and Institute für Chemische Technologie, Universität Stuttgart, 70550-Stuttgart, Germany

Received: March 19, 1997; In Final Form: June 30, 1997[⊗]

Two novel medium pore cobalt-substituted aluminophosphate molecular sieves CoAPO-41 and CoAPSO-41 have been synthesized hydrothermally using di-*n*-propylamine as the organic template. These materials have been characterized by various physical methods including XRD, TGA, SEM, electron microprobe analysis, ^{27}Al, ^{29}Si, and ^{31}P MAS NMR, UV−visible, and ESR spectroscopies. Substitution of cobalt into the framework has been established. Cobalt in CoAPO/CoAPSO-41 after calcination in O_2 and subsequent dehydration and H_2 treatment at high temperature activates molecular oxygen by forming a peroxocobalt adduct Co−O−O•. The peroxo species is unstable at temperatures above 573 K. Adsorption of molecules such as D_2O, ND_3, CH_3OD, and CO on CoAPO/CoAPSO-41 materials after calcination, dehydration, and high-temperature hydrogen treatment forms complexes with Co(II) from the framework as revealed by ESR measurements at 4.5 and 77 K.

Introduction

Transition-metal-incorporated aluminophosphate molecular sieves have gained considerable significance during the past several years due mainly to the bifunctional characteristics of such materials in several catalytic reactions.[1] Cobalt-substituted aluminophosphate (CoAPO) and silicoaluminophosphate (CoAPSO) molecular sieves are particularly interesting compounds in reactions such as autoxidation of *p*-cresol and cyclohexane.[2] Framework substitution of cobalt and other divalent metals has been reported in several structure types.[3] Most of the studies have been focused on structure types 5 (AFI), 11 (AEL), 20 (SOD), and 34 (CHA). These materials can be readily synthesized with a number of organic molecules as structure-directing agents. The structure type 41 (AFO) is a less widely studied medium pore molecular sieve with 10 tetrahedral (T) atom pore openings. The AFO framework topology consists of elliptical one-dimensional 10-ring channels that are slightly larger than the 10-ring channels in the AEL structure type.[4] SAPO-41 molecular sieve has been shown to be highly active for the alkylation of toluene.[5] The activity is shown to be higher than that of the well-known catalyst H−ZSM-5, although the selectivity patterns exhibited by these materials are different. Metal substitution in the AFO framework has not been studied until recently; we reported the synthesis and characterization of NiAPSO-41 molecular sieve.[6] In the present study, we report the synthesis of CoAPO-41 and CoAPSO-41 molecular sieves and the characterization of such materials by various spectroscopic techniques.

Experimental Section

Synthesis. CoAPO-41 and CoAPSO-41 were prepared hydrothermally using di-*n*-propylamine as the organic template. Samples of $AlPO_4$-41 and SAPO-41 were also prepared following the procedure reported elsewhere.[5] The following chemicals were used without further purification: orthophosphoric acid (85%, Mallinckrodt), pseudoboehmite (Catapal-B, Vista), fumed silica (Sigma), di-*n*-propylamine (98%, Aldrich), and cobalt acetate tetrahydrate (Aldrich). Syntheses were carried out in 20 cm^3 stainless steel reactors lined with polytetrafluoroethylene at autogenous pressure without agitation. Based on preliminary experiments, the following molar compositions were optimized for the synthesis of pure CoAPO-41 and CoAPSO-41 molecular sieves:

CoAPO-41: $0.3CoO:0.98Al_2O_3:1.25P_2O_5:4.0R:55H_2O$

CoAPSO-41:
$0.3CoO:0.98Al_2O_3:0.1SiO_2:1.25P_2O_5:4.0R:55H_2O$

where R is di-*n*-propylamine. In a typical synthesis of CoAPSO-41, 3.59 g of pseudoboehmite is slurried in 6 g of H_2O and stirred for 2 h. Then 0.19 g of cobalt acetate dissolved in 5 g of H_2O is mixed with 6.92 g of phosphoric acid diluted in 5 g of H_2O, and the solution is added dropwise to the alumina slurry . The mixture is stirred for 4 h. Fumed silica (0.15 g) is then added. After stirring for 30 min, 10.12 g of di-*n*-propylamine is added dropwise to the mixture. The pH of the gel is adjusted at 7.8 by adding 1.15 g of phosphoric acid diluted with 6.6 g of H_2O. About 50 mg of finely ground $AlPO_4$-41 crystals is then added to the gel as seed crystals. The final gel is aged for 18 h at 295 K under stirring. About 10 mL of the gel is put into each of three autoclaves and kept at 473 K for 24 h. After crystallization, the product is separated from the mother liquor, washed with water, and dried at 353 K overnight. The as-synthesized sample is calcined by raising the temperature slowly to 823 K in N_2 and then keeping the sample at this temperature for 16 h in O_2 for removal of the organic template.

Sample Treatment and Measurements. X-ray powder diffraction patterns were recorded on a Philips PW1840 diffractometer using Cu Kα radiation. Thermogravimetric (TG) analysis were carried out in O_2 on a Dupont 957 thermal analyzer at a heating rate of 10 K/min. Chemical analysis of the samples were carried out by electron probe microanalysis, and morphology and particle size of the samples were studied by scanning electron microscopy on a Jeol JXA -8600 spectrometer. The surface areas of the samples were obtained on a

[†] University of Houston.
[‡] Universität Stuttgart.
* To whom correspondence should be addressed.
[⊗] Abstract published in *Advance ACS Abstracts,* August 15, 1997.

S1089-5647(97)00993-0 CCC: $14.00

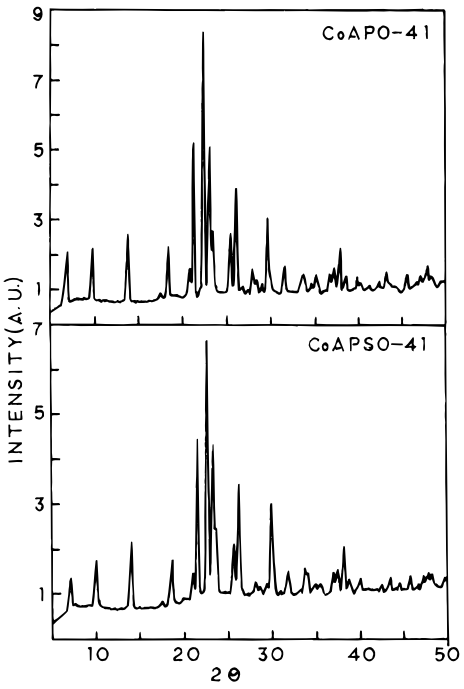

Figure 1. X-ray powder diffraction pattern of as-synthesized CoAPO-41 (top) and CoAPSO-41 (bottom).

Quantchrome Instrument using a single-point BET surface area method. Electronic absorption spectra were recorded on a Perkin-Elmer 330 UV−visible spectrophotometer using quartz as a reference sample. Solid state MAS NMR spectra were obtained on a Bruker MSL 400 spectrometer using a 4 mm zirconia rotor with a KF cap spun at a frequency of 10 kHz. The ^{31}P spectroscopic data on the hydrated samples were obtained at a frequency $w_0/2p = 161.91$ MHz with a recycle delay of 30 s with 85 wt % H_3PO_4 used as a reference. The ^{27}Al MAS NMR spectra were obtained at $w_0/2p = 104.26$ MHz with a recycle delay of 1 s with the spectra referenced against $Al(H_2O)_6^{3+}$.

For ESR measurements the as-synthesized and calcined samples were loaded into 3 mm o.d. by 2 mm i.d. Suprasil quartz tubes and evacuated to a final pressure of 10^{-4} Torr. ESR spectra were measured at both 4.5 and 77 K. In order to prepare Co(II) complexes with various adsorbates, the calcined samples were dehydrated in vacuum by gradually raising the temperature from room temperature (RT) to 773 K over a period of 8 h and kept at that temperature for 24 h. The sample was then brought back to RT, exposed to 2 atm of H_2, and heated to 673 K for 2 days (activation). The green color of the original calcined sample was changed to pale blue after this activation treatment. Samples were evacuated for 1 h before exposing to 10 Torr of O_2, 100 Torr of CO (MSD isotopes), 70 Torr of ND_3 (Stohler isotope Chemicals), and the room temperature vapor pressure of D_2O (Aldrich). These samples with adsorbates were sealed and stored at RT for a long period before ESR measurements. ESR spectra at 4.5 and 77 K were recorded with a Bruker ESP 300 X-band spectrometer operated with 100 kHz frequency modulation. The spectrometer was equipped with an Oxford Instruments ESR 900 liquid helium, continuous-flow cryostat. The temperature of the sample was determined with a Au−Fe/chromel thermocouple calibrated in liquid nitrogen at atmospheric pressure. The magnetic field was calibrated with a Varian E-500 gaussmeter. The microwave frequency was measured by a Hewlett-Packard HP 5342A frequency counter.

Results

Synthesis. In the synthesis of CoAPO-41 and CoAPSO-41, crystals of $AlPO_4$-41 were employed as seeds. A pure phase can only be obtained with a relatively low concentration of cobalt (0.01−0.05 mol) in the synthesis gel. As-synthesized CoAPO-41 and CoAPSO-41 were blue. At higher cobalt concentration, a dense phase started crystallizing along with the AFO phase, and the color of the sample changed from blue to pink. Samples were characterized by XRD. Figure 1 shows the powder XRD pattern of as-synthesized CoAPO-41 and CoAPSO-41. These patterns, in both intensity and line position, match well with the patterns reported for structure type 41.[7,8] No extra peaks or peak broadening was observed in CoAPO-41 or CoAPSO-41. Scanning electron microscopic analysis of the various products verified the crystallinity and phase purity of these samples (Figure 2). Both CoAPO-41 and CoAPSO-41 crystallize with rectangular morphology with size varying from 5 to 12 μm. AlPO-41 and SAPO-41 crystallize in the same morphology but with smaller crystallite size in the range 1−2 and 5−8 μm, respectively. Electron microprobe analysis of the various products gave the following chemical compositions.

$AlPO_4$-41: $(Al_{0.51}P_{0.49})O_2$

SAPO-41: $(Si_{0.02}Al_{0.51}P_{0.47})O_2$

CoAPO-41: $(Co_{0.03}Al_{0.47}P_{0.50})O_2$

CoAPSO-41: $(Co_{0.02}Al_{0.48}P_{0.48}Si_{0.02})O_2$

The surface areas measured for these four samples are 161, 136, 145, and 139 m^2/g for $AlPO_4$-41, SAPO-41, CoAPO-41, and CoAPSO-41, respectively. These values are somewhat higher than the corresponding value reported for SAPO-11 (123 m^2/g), but substantially lower than for SAPO-5 (214 m^2/g) and consistent with the pore size differences of these various structure types. The somewhat higher surface area obtained for $AlPO_4$-41 may be due to a higher crystallinity for this sample.

To investigate the thermal properties of the various AFO compositional variants, thermogravimetric analysis in flowing O_2 of as-synthesized AlPO-41, SAPO-41, CoAPO-41, and CoAPSO-41 were carried out, and the results are shown in Figure 3. The initial small weight loss up to 400 K is due to the desorption of physically adsorbed water. The desorption of the organic template takes place in a single step in $AlPO_4$-41 and in multisteps in SAPO-41, CoAPO-41, and CoAPSO-41. The low-temperature weight loss around 473 K in all the compositional variants is tentatively assigned to decomposition of dipropylamine occluded inside the channels. The high-temperature weight loss is assigned to the desorption and decomposition of protonated amines, balancing the framework negative charge.[9] The high-temperature weight loss is more prominent in SAPO-41 and CoAPSO-41 than in CoAPO-41. Being a neutral framework, $AlPO_4$-41 does not require any protonated amines in its channels, which explains the absence of such a high-temperature weight loss in this material. The high-temperature weight loss observed in SAPO-41 and CoAPSO-41 is higher than the corresponding weight loss reported for SAPO-11.[10] This is likely due to a larger number of acid sites in SAPO-41 materials compared to SAPO-11. The AFO structure remains stable up to 973 K under controlled heating conditions, although loss in crystallinity is observed after heating the sample above 823 K for a prolonged period.

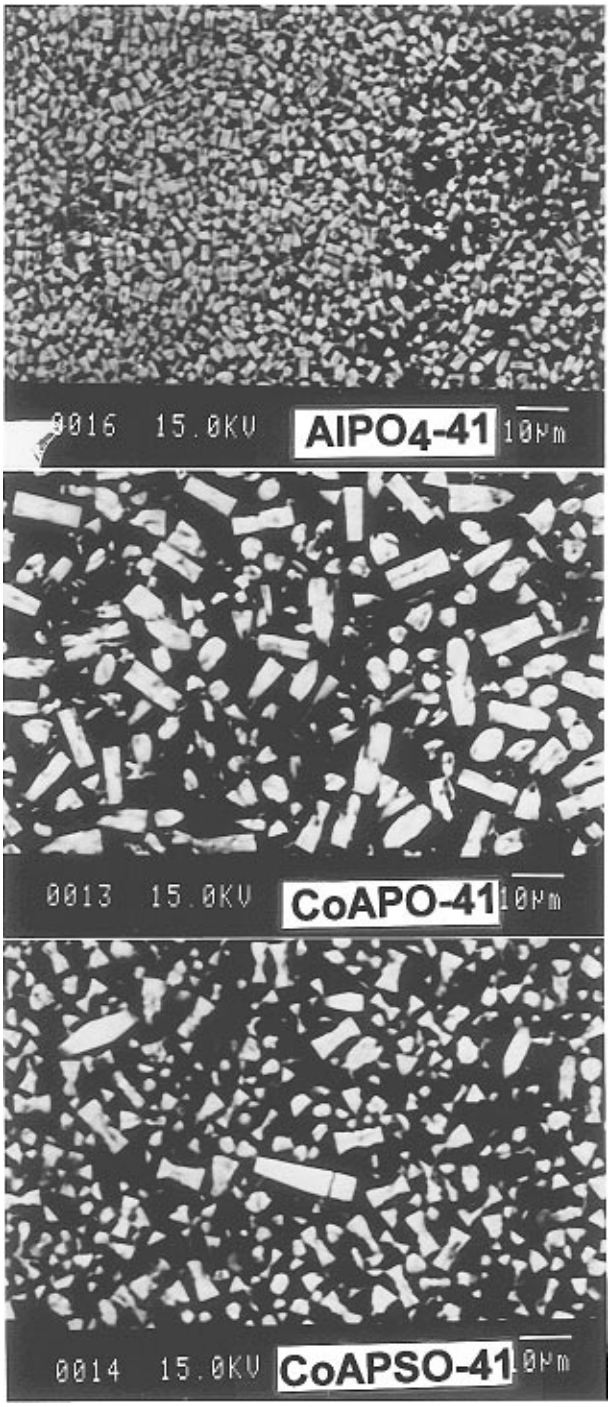

Figure 2. Electron micrographs of $AlPO_4$-41 (top), CoAPO-41 (middle), and CoAPSO-41 (bottom) molecular sieves. Scale bar is 10 μm.

Solid State MAS NMR. The ^{31}P NMR spectra of hydrated, as-synthesized SAPO-41 and CoAPSO-41 exhibit a single line at −30.9 and −30.7 ppm, respectively (Figure 4), consistent with tetrahedral phosphorus in the $AlPO_4$ framework.[11] As-synthesized $AlPO_4$-41 and CoAPO-41 exhibit four peaks within the chemical shift region of −19 and −37 ppm in the ^{31}P spectrum as shown in Figure 5. In $AlPO_4$-41 a small signal at −11.4 ppm is also observed. Deconvolution of the spectra gave relative intensity ratios for the various peaks (from low field to high field) of 9:19:67:5 for CoAPO-41 and 3: 4:21:69:3 for $AlPO_4$-41. The major ^{27}Al peak around 38 ppm for CoAPO-41 and CoAPSO-41 (Figure 6) is in agreement with our data and previous literature data for the parent materials AlPO-41 and SAPO-41.[4,5,12] These values are consistent with aluminum being in tetrahedral coordination. No extraframework octahedral aluminum was detected in our samples. The ^{29}Si MAS NMR spectrum (not shown) of CoAPSO-41 shows a broad resonance in the region from −90 to −115 ppm, indicating multiple silicon environments in the framework.

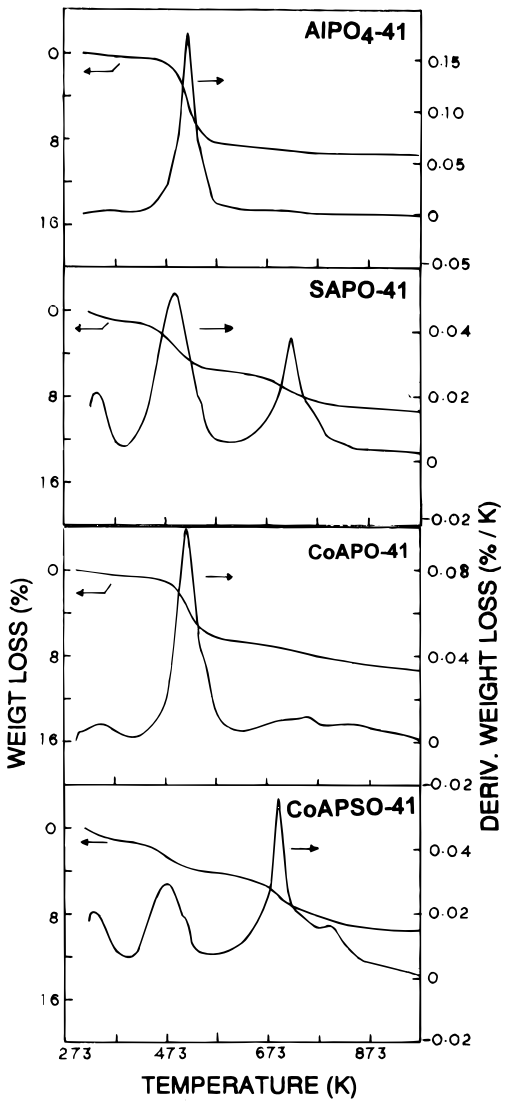

Figure 3. Thermogravimetric analysis curves of as-synthesized $AlPO_4$-41, SAPO-41, CoAPO-41, and CoAPSO-41 molecular sieves.

Electronic absorption spectra of both CoAPO-41 and CoAPSO-41 are the same as reported earlier for other CoAPO-*n* and CoAPSO-*n* molecular sieves.[13,14] The spectra show absorption bands in the 500−650 nm region due to tetrahedral Co(II).[13] When as-synthesized samples are calcined in O_2, the intensity of this band region decreases with concomitant formation of a broad band in the 250−450 nm region. These spectral changes agree with previous work.

Figure 7 shows the ESR spectra recorded at 4.5 and 77 K for CoAPSO-41 as-synthesized, calcined, and dehydrated and after hydrogen treatment of a dehydrated sample at 723 K. Both CoAPO-41 and CoAPSO-41 give similar ESR spectra with respect to the various pretreatments of the samples. A single species A with $g_\perp = 6.0$ and $g_\parallel = 2.0$ is observed in as-synthesized samples. After calcination the intensity of this signal reduces considerably. Upon hydrogen treatment at high temperature, the intensity of this signal again increases as shown in Figure 7c. This signal has been previously assigned to high-spin Co(II) in a distorted tetrahedral environment.[15] The spectra of the sample after calcination and hydrogen treatment are

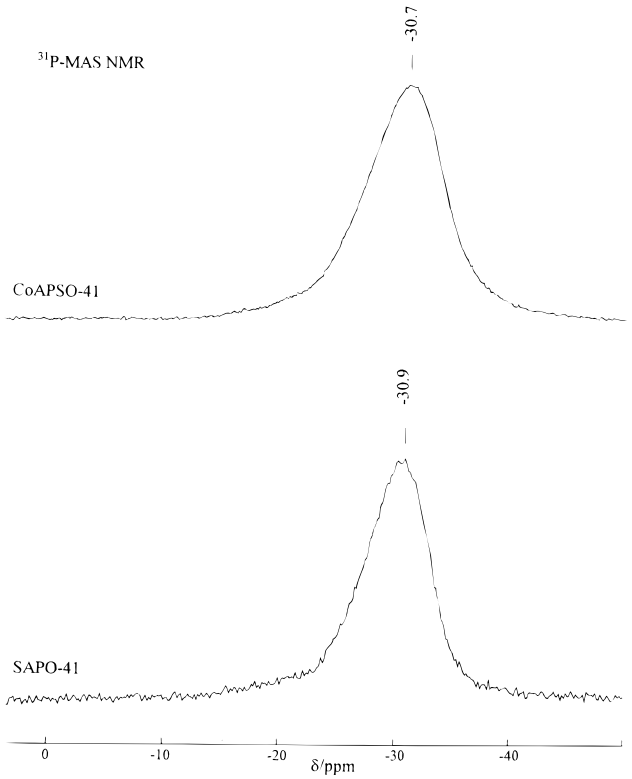

Figure 4. ^{31}P MAS NMR spectra of as-synthesized SAPO-41 (bottom) and CoAPSO-41 (top) molecular sieves.

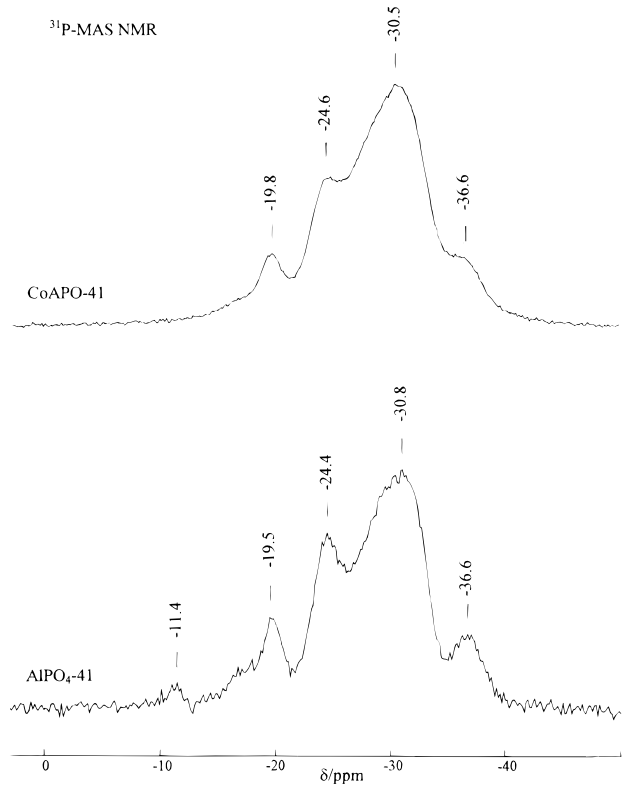

Figure 5. ^{31}P MAS NMR spectra of as-synthesized AlPO$_4$-41 (bottom) and CoAPO-41 (top) molecular sieves.

broadened compared with that before calcination, probably due to differences in relaxation parameters and/or to interaction with oxygen and hydrogen. In calcined and hydrogen-treated samples a small species B with $g_\perp = 2.06$ is also observed. When measured at 77 K, the spectra show some differences (Figure 7d−f). Species B is absent. Species C with $g = 2.005$ is assigned to an organic radical generated during thermal

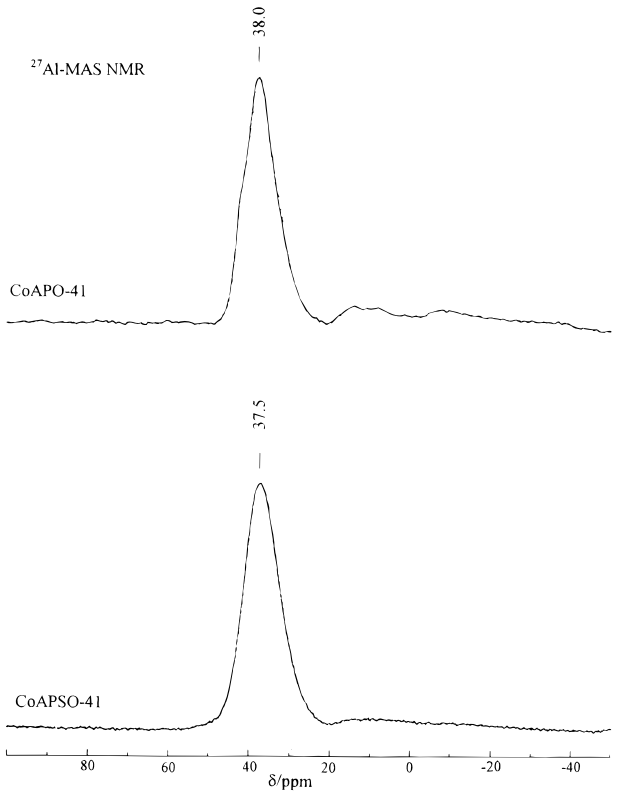

Figure 6. ^{27}Al MAS NMR spectra of as-synthesized CoAPO-41 (top) and CoAPSO-41 (bottom) molecular sieves.

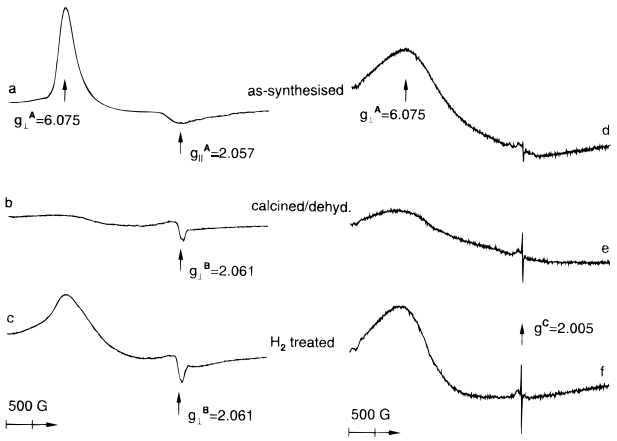

Figure 7. ESR spectra at 4.5 K (left) and 77 K (right) of CoAPSO-41 as-synthesized (a, d), calcined, and dehydrated (b, e) and after hydrogen treatment at 723 K of the calcined, dehydrated sample (c, f).

decomposition of the template. Although the band around $g = 6.0$ is still visible, the intensity reduces considerably.

The effect of the addition of oxygen to an activated sample showing Co(II) signals was also studied. No new ESR signal is observed when a calcined and dehydrated sample is contacted with molecular oxygen. However, a strong ESR signal with anisotropic g values $g_1 = 2.022$, $g_2 = 2.010$, and $g_3 = 2.004$ is observed (species D in Figure 8) when an activated sample is contacted with O_2 at 473 K. This signal has been previously identified as cobalt superoxide ion.[16] The pretreatment (activation) of the sample before adsorption of O_2 is found to be critical in producing this signal. The signal is observed only after O_2 adsorption on a sample that is previously treated with H_2 at 673 K or above for a prolonged period. The thermal stability of these superoxide ions is found to depend on the sample temperature. As shown in Figure 8b,c, annealing the sample above 473 K reduces the signal intensity, and the signal

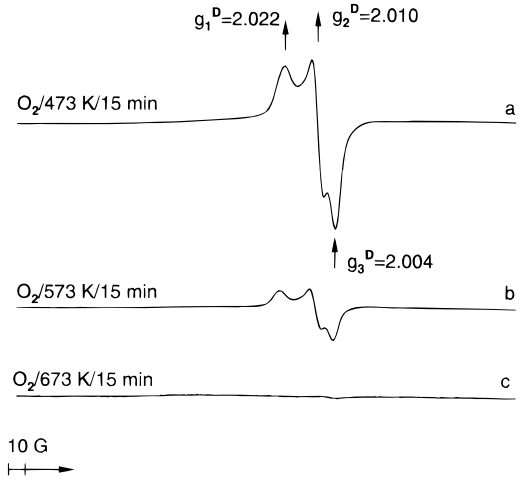

Figure 8. ESR spectra at 77 K after O_2 (10 Torr) adsorption on a calcined, dehydrated, and H_2-treated sample of CoAPSO-41 and after annealing the sample for 15 min at 473 (a), 573 (b), and 673 K (c).

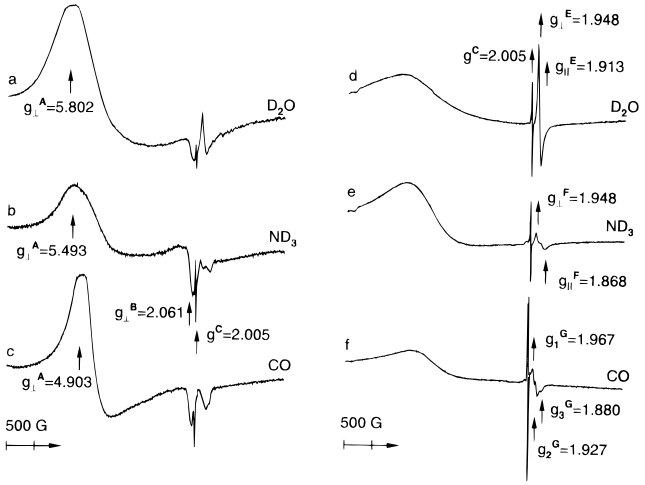

Figure 9. ESR spectra at 4.5 K (left) and 77 K (right) after adsorbing D_2O (a, d), ND_3 (b, e), and CO (c, f) on CoAPSO-41 after calcination, dehydration, and H_2 treatment.

completely disappears at 673 K. The signal can be reproduced only after hydrogen treatment of the sample at high temperature followed by the addition of O_2 at 473 K.

Figure 9 shows ESR spectra measured at 4.5 and 77 K after adsorption of D_2O, ND_3 and CO on activated CoAPSO-41 samples. The characteristic feature of these spectra is the formation of new species with g values below 2, which is apparently due to the coordination of these molecules to Co(II). The signal at $g = 2.06$ is absent when measurements are done at 77 K. With D_2O, species E with axially symmetric components $g_{||} = 1.913$ and $g_\perp = 1.948$ is observed. With ND_3, a new species F with $g_{||} = 1.868$ and $g_\perp = 1.948$ is observed with weaker intensity than species E. Adsorption of CO, however, gives species G with rhombic g components ($g_1 = 1.967$, $g_2 = 1.927$, and $g_3 = 1.880$). The g characteristics of species A are also modified to different extents after adsorption of various molecules.

Discussion

The organic molecule dipropylamine templates at least nine structure types having a wide range of pore openings in the synthesis of aluminophosphate-based molecular sieves from extra large pore VPI-5 to small pore $AlPO_4$-39.[9] Thus, optimizing the synthesis parameters for a given structure type to crystallize pure materials is extremely difficult. The gel composition, pH, temperature, and duration of heating influence the crystallinity and purity of these structures. Some systematic studies have been reported on the preparation of some of these structure types in the presence of dipropylamine by varying the synthesis conditions and gel composition.[3,9] Structure type 41 was reported to be crystallized from a gel having a high concentration of organic template and a low silicon or metal concentration. Similar conditions were observed for the synthesis of CoAPO-41 and CoAPSO-41. However, these materials can only be prepared as pure phases by adding seed crystals of $AlPO_4$-41 to the gel prior to heating. Our attempts to prepare this material without seed crystals were not successful. On the other hand, both $AlPO_4$-41 and SAPO-41 can be prepared without seed crystals in the gel, but a long period of heating at a relatively lower temperature of 453 K is required. By adding seed crystals, the period of crystallization for both $AlPO_4$-41 and SAPO-41 is reduced considerably. The effect of adding seed crystals to a synthesis batch is to increase the crystallization rate by providing more surface area for the assimilation of nutrient material from solution and shortening the time required for crystallization to be completed.[17] However, the exact mechanism of nucleation in a seeded system is not yet fully understood.

The X-ray powder diffraction patterns of CoAPO-41 and CoAPSO-41 in both intensity and line position match well with the patterns of $AlPO_4$-41 and SAPO-41. No peak broadening is observed between these compositional variants. A significant color difference depending on the location of cobalt ion in tetrahedral framework sites or in ion-exchanged sites has been demonstrated previously for CoAPO-*n* materials.[13] When Co(II) is added during synthesis to form CoAPO-41 and CoAPSO-41, the product is blue. After calcination of the samples at 823 K, the color changes to yellow-green. It is observed that when cobalt is ion-exchanged into AlPO-41 or SAPO-41, the exchanged material is violet (rather than blue) and turns to gray after high-temperature O_2 treatment.

The TGA data for $AlPO_4$-41 and SAPO-41 are different from those of CoAPO-41 and CoAPSO-41. The extra step at high temperature involved in the combustion of the templating agent in SAPO-41 and CoAPSO-41 suggests that part of the dipropylamine is protonated in these samples. The high-temperature weight loss is less in CoAPO-41 than in SAPO-41 and CoAPSO-41 for the obvious reason that Si in the SAPO-41 and CoAPSO-41 samples is mostly responsible for this weight loss as follows. Depending on the mechanism of substitution of silicon and metal ions, one or more net framework charges will be created which can be balanced by protonated amine. The high-temperature template weight loss is higher in CoAPSO-41 (5.4 wt %) than in SAPO-41 (3.6 wt %), which suggests the presence of additional acid sites in CoAPSO-41 due to the incorporation of metal in the framework. Correspondingly, the low-temperature template weight loss is higher in SAPO-41 (4.6 wt %) than in CoAPSO-41 (2.8 wt %). Note that both materials were prepared with the same amount of silica and di-*n*-propylamine in the synthesis gel.

Isomorphous substitution of silicon into the $AlPO_4$ framework can be visualized in terms of silicon substituting only aluminum (mechanism 1), only phosphorus (mechanism 2), or a phosphorus−aluminum pair (mechanism 3). It has been generally accepted that mechanisms 2 and 3 are responsible for the formation of SAPO structures.[18] The mechanism of silicon substitution depends on the topology of the framework and on the method of synthesis. A recent study on the mechanism of silicon substitution in SAPO-41 by ^{29}Si MAS NMR and temperature-programmed desorption of ammonia revealed that

mechanism 2 is prominent in this structure, whereas in other medium pore SAPO structures such as SAPO-11 and SAPO-31, mechanism 3 is predominant. It should be noted that while mechanism 2 produces a net negative framework charge, mechanism 3 does not. Incorporation of a divalent metal ion into a basic aluminophosphate framework can proceed either by replacing an aluminum or phosphorus from the framework. On the basis of various structural and elemental analysis results, it has been suggested that metal ions replace aluminum from the framework.[3] However, recent electron spin echo modulation studies on Ni-substituted SAPO-5 and SAPO-11 suggest that Ni ions replace phosphorus ions from the framework.[19] Thus, depending on the type of substitution, incorporation of a divalent metal ion into a basic aluminophosphate framework can generate either one or two framework negative charges. The framework negative charge generated by the substitution of silicon for phosphorus is normally balanced by protonated amine in the as-synthesized form and by H^+ ions in the calcined form. The framework compositions of the CoAPO-41 and CoAPSO-41 materials suggest that cobalt substitutes for framework aluminum. In an ideal CoAPO framework where cobalt substitutes for aluminum sites, the ratio (Al + Co)/P should be unity. This is indeed the case observed. Similarly in CoAPSO molecular sieves, the ratio (Al + Co)/(P + Si) should be unity if silicon substitution is entirely by mechanism 2 and cobalt substitutes for aluminum sites. However, the observation that this ratio is unity in our CoAPSO-41 does not exclude the possibility of two silicon atoms substituting for a Al−P pair (mechanism 3). In fact, in most SAPO and MeAPSO molecular sieves, the so-called pairwise substitution of silicon to create "silica islands" within the molecular sieve framework is a common occurrence as evidenced from ^{29}Si MAS NMR results.[18,20,21] In particular, in MeAPSO molecular sieves, the metal ions in the framework seem to avoid silicon as their nearest-neighbor tetrahedral atoms forcing silicon to form silica islands. Our ^{29}Si MAS NMR results also suggest a similar situation in CoAPSO-41. Instead of a sharp resonance at −93 ppm observed in SAPO-41,[5] only a broad resonance between −88 and −115 ppm is observed in CoAPSO-41. The broad resonance is indicative of multiple tetrahedral silicon environments and further suggests that silicon enters into framework by both mechanism 2 and mechanism 3, thereby forming isolated $Si(OAl)_4$ sites and silica-rich regions.

^{31}P MAS NMR of both $AlPO_4$-41 and CoAPO-41 show a broad resonance with four peaks in the range −19 to −37 ppm, whereas SAPO-41 and CoAPSO-41 show only a single resonance peak at −30.9 and −30.7 ppm, respectively. Considering the four crystallographically distinct T sites existing in $AlPO_4$-41,[4] it is tempting to assign the observed four peaks to phosphorus at these different sites. However, it has been reported that, in calcined and not rehydrated $AlPO_4$-41, only a single resonance at −31.5 ppm is observed, suggesting that the various crystallographic sites are not resolved in a calcined sample.[4,12] Furthermore, if one assumes a nonpreferential distribution of phosphorus over these sites, one expects intensity ratios of 20:20:40:20 for the four peaks in the NMR. These ratios are different from the observed ratios.

In $AlPO_4$-31, an aluminophosphate synthesized with di-*n*-propylamine which contains a unique T site, a single resonance around −30 ppm is observed in as-synthesized and calcined samples.[22] The effect of template removal and dehydration is to shift the resonance line to higher field in comparison to that of as-synthesized materials, suggesting influence of the templating molecules on the Al and P environment or on the Al−O−P angle.[23] VPI-5 and $AlPO_4$-11 prepared with di-*n*-propylamine contain more than one crystallographically independent site. There, ^{31}P MAS NMR spectra show multiple signals due to different P sites and also due to interaction with extraframework molecules.[1,24] Thus, the observed multiple NMR peaks for ^{31}P in as-synthesized AlPO-41 and CoAPO-41 are probably due to the combined effects of crystallographically independent T sites and the interaction of the P atoms with template and/or water molecules to varying extents. Incorporation of silicon in framework phosphorus sites creates a negative charge which is balanced by protonated amines. In SAPO-41 and CoAPSO-41 it is likely that the protonated amines are located within the large channel at sites near Si ions and hence reduce the interaction between phosphorus and the organic ions. The absence of multiple signals in SAPO-41 and CoAPSO-41 may be explained this way. However, further detailed studies are necessary for better understanding of these observations. The slightly increased line width in the Co-containing materials is in agreement with the existence of paramagnetic Co(II) in the samples.

The ^{27}Al MAS NMR spectrum of aluminophosphate molecular sieves is generally consistent with tetrahedral framework $Al(OP)_4$ modified by second-order quadrupole coupling effects and interaction with entrapped template or water in the adjacent channels. Crystallographically independent sites are normally not resolved in a ^{27}Al MAS NMR spectrum for AlPO materials. The ^{27}Al MAS NMR spectra for all the compositional variants show a single resonance near 38 ppm characteristic of tetrahedral Al in the framework. These observations are consistent with earlier results on other $AlPO_4$ type molecular sieves.[11,22] As expected, aluminum ions occupying crystallographically distinct T sites are not resolved in the ^{27}Al MAS NMR spectra.

From the known structure of $AlPO_4$-41 it is logical to assume that if Co(II) ions substitute into the $AlPO_4$ framework, they will be in a tetrahedral environment replacing some lattice Al ions as suggested by the chemical analysis results. The resulting tetrahedral crystal field experienced by Co(II) should give a high-spin electron configuration and a very short spin−lattice relaxation time so that very low temperature would be needed to detect the signal. ESR behavior of high spin Co(II) in a variety of coordination complexes has been studied previously.[25]

The g value observed for Co(II) species A in as-synthesized CoAPO-41 and CoAPSO-41 is characteristic of Co(II) in a tetrahedral or more probably a distorted tetrahedral environment. Calcination in O_2, however, reduces the intensity of this signal significantly. A much broader ESR signal with $g_\perp \sim 6.0$ reappears when a calcined sample is treated with H_2 at high temperature. Similar behavior has been observed in other CoAPO molecular sieves. Initially, this was interpreted as due to a Co(II)/Co(III) oxidation−reduction cycle of the framework cobalt.[26] However, from a detailed study of the ESR temperature dependence of CoAPO-5 , Kurshev et al.[15] showed that the observed changes in the ESR behavior are not due to the oxidation−reduction behavior of framework cobalt, but rather to a reversible lattice distortion caused by interaction with oxygen molecules.

In a recent study on CoAPO-11 molecular sieve, Naccache et al.[16] reported that both O_2-calcined and H_2-treated samples exhibited similar behavior for reaction with pyridine. Both samples showed similar infrared spectra before and after adsorption of pyridine, indicating that their proton acidity is the same. Isomorphous substitution of Co(II) for trivalent Al in $AlPO_4$ generates a negative framework charge balanced by protonated amine in as-synthesized and H^+ in calcined samples. On the other hand, no proton acidity is expected in a CoAPO framework where Co is present as Co(III). A possible reaction scheme has been suggested for the observed ESR behavior of

as-synthesized, calcined, and H_2-treated samples as follows.

$$\text{as-synthesized CoAPSO-41:} \quad Co^{2+}(\text{template})$$

$$\text{calcination in } O_2\text{:} \quad Co^{2+}(\text{template}) + O_2 \rightarrow (Co{=}O)^{2+}$$

$$H_2 \text{ treatment at 673 K:} \quad (Co{=}O)^{2+} + H_2 \rightarrow Co^{2+} + H_2O$$

This reaction scheme not only explains the same proton acidity observed for calcined and H_2-treated samples but also explains why CoAPO-41 and CoAPSO-41 activate molecular oxygen only after H_2 treatment of a calcined sample. For an H_2-treated sample, tetrahedral Co(II) can form a bond with O_2 via coupling of one unpaired d electron of Co(II) and one unpaired π electron of molecular oxygen, forming a covalent peroxo cobalt adduct Co−O−O• (Figure 8a). At high temperature, the peroxocobalt adduct is converted to Co═O again, which is inactive toward activation of molecular oxygen and hence explains the reduction in ESR signal intensity at high temperatures (Figure 8b,c).

Co(II) species B observed in calcined and H_2-treated samples is probably due to framework cobalt having additional coordination with molecular oxygen. In support of this assumption, an ESR signal with $g_1 = 2.060$, $g_2 = 2.088$, and $g_3 = 2.188$ for a low-spin $[Co(II)(terpy)_2]^{2+}$ complex, where Co(II) is hexacoordinated by two tridentate 2,2,2-terpyridine (terpy) ligands, has been reported in zeolite Y.[27] A signal with g values of $g_\perp = 2.062$ and $g_{||} = 2.258$ was reported for a low-spin five-coordinate Co(II) complex $[CoCl(dpe)_2]SnCl_3 \cdot C_6H_5Cl$, where dpe represents 1,2-bis(diphenylphosphineo).[28] Almost similar g values were reported for a number of complexes $[CoX(dpe)_2]Y$, where X and Y are Cl^-, Br^-, NO_3^-, ClO_4^-, anions, etc.[29] The fact that species B is not observed at 77 K suggests a short spin−lattice relaxation time which is quite uncommon among low-spin cobalt complexes. Assigning species B to extraframework Co(II) is unlikely because species B is not observed in as-synthesized samples. A similar Co(II) species B is not observed when Co(II) is ion-exchanged into SAPO or ZSM-5 materials.

The various species observed after adsorption of D_2O, ND_3, and CO on CoAPSO-41 indicate that Co(II) complexes are formed with these molecules. The **g** tensors of species E, F, and G and the fact that these species can be observed at 77 K are characteristic of low-spin Co(II) complexes with five- or six-coordinate geometry. The signal due to tetrahedral Co(II) (species A) is also modified to varying extents by adsorption of these molecules.

Measurement at room temperature does not show any ESR signals. Several ESR studies on low-spin octahedral cobalt(II) complexes have been reported in the literature.[30] Dioxygen-binding Co(II) complexes have been formed within the cages of zeolites with neutral or anionic ligands like amines, cyanide, bipyridine, and terpyridine.[31] Such complexes are generally ESR detectable low-spin Co(II) species. ESR studies of adsorbate interactions of cobalt(II) in the framework of microporous solids are not available in the literature. Adsorbate interactions of paramagnetic ions such as Mn(II) and Ni(I) in the framework of $AlPO_4$-based molecular sieves have been previously studied by a combination of ESR and electron spin echo modulation spectroscopy.[32,33] For adsoption of D_2O on MnAPO-11, two molecules of D_2O coordinate with Mn(II) in the framework. On the other hand, only one molecule of CD_3OH or C_2D_4 coordinates with Mn(II) in the framework. Similarly, one molecule of CD_3OH and C_2D_4 coordinates with framework Ni(I) in NiAPSO-11 material. Thus, a similar situation is expected for framework Co(II) where the geometrical constraints of the molecular sieve framework restrict the number of coordinating adsorbate molecules to Co(II) to be one or two. Electron spin echo modulation of Co(II) has not been successful so we have not been able to quantify the framework Co(II) adsorbate coordination. However, from a combined UV−vis and FTIR spectroscopic study on the adsorption of C_2H_4, CO, and H_2O on CoAPO-18, Marchese et al.[34] concluded that framework Co(II) interacts with one molecule of these adsorbates.

Conclusions

Hydrothermal synthesis of CoAPO-41 and CoAPSO-41 molecular sieves has been achieved using di-*n*-propylamine as the structure-directing agent. Synthesis parameters for pure and highly crystalline samples have been optimized. The materials were characterized by various physicochemical methods. Cobalt substitution in the aluminophosphate framework has been confirmed. Activation of CoAPO-41 and CoAPSO-41 by calcination in O_2, dehydration, and H_2 treatment at high temperature form a peroxocobalt adduct upon adsorption of molecular oxygen. Framework Co(II) in CoAPO-41 and CoAPSO-41 forms complexes with D_2O, CO, and ND_3 upon adsorption on activated samples.

Acknowledgment. This research was supported by the National Science Foundation and the Robert A. Welch Foundation.

References and Notes

(1) Vedrine J. C. In *Zeolite Chemistry and Catalysis*; Jacobs, P. A., Jaeger, N. I., Kubelkova, L., Wichterlova, B., Eds.; Studies in Surface Science and Catalysis, Vol. 69; Elsevier: Amsterdam, 1991; pp 25−42.
(2) Lin, S. S.; Weng, H. S. *Appl. Catal. A* **1993**, *105*, 289.
(3) Wilson, S. T.; Flanigen, E. M. In *Zeolite Synthesis*; Occelli, M. L., Robson, H. E., Eds.; ACS Symposium Series, Vol. 398; American Chemical Society: Washington, DC, 1989; pp 329−345.
(4) Kirchner, R. M.; Bennett, J. M. *Zeolites* **1994**, *14*, 523.
(5) Prakash, A. M.; Chilukuri, S. V. V.; Bagwe, R. P.; Ashtekar, S.; Chakrabarty, D. K. *Microporous Mater.* **1996**, *6*, 89.
(6) Prakash, A. M.; Hartmann, M.; Kevan, L. *J. Chem. Soc., Faraday Trans.* **1997**, *93*, 1233.
(7) Wilson, S. T.; Lok, B. M.; Flanigen, E. M. U.S. Patent 4 310 440, 1982.
(8) Lok, B. M.; Messina, C. A.; Patton, R. L.; Gajek, R. T.; Cannan, R. T.; Flanigen, E. M. U.S. Patent 4 440 871, 1984.
(9) Ojo, A. F.; McCusker, L. B. *Zeolites* **1991**, *11*, 460.
(10) Azuma, N.; Lee, C. W.; Kevan, L. *J. Phys. Chem.* **1994**, *98*, 1217.
(11) Blackwell, C. S.; Patton, R. L. *J. Phys. Chem.* **1988**, *92*, 3965.
(12) Clark, H. W.; Rievert, W. J.; Olken, M. M. *Microporous Mater.* **1996**, *6*, 115.
(13) Kraushaar-Czarnetzki, B.; Hoogervorst, W. G. M.; Andrea, R. R.; Emeis, C. A.; Stork, W. H. J. *J. Chem Soc., Faraday Trans.* **1991**, *87*, 891.
(14) Prakash, A. M.; Chilukuri, S. V. V.; Ashtekar, S.; Chakrabarty, D. K. *J. Chem. Soc., Faraday Trans.* **1996**, *92*, 1257.
(15) Kurshev, V.; Kevan, L.; Parillo, D. J.; Kokotailo, G. T.; Gorte, R. J. *J. Phys. Chem.* **1994**, *98*, 10160.
(16) Naccache, C.; Vishnetskaya, M.; Chao, K.-J. In *Progress in Zeolite and Microporous Materials*; Chon, H., Kilhm, S., Uh, Y. S., Eds.; Studies in Surface Science and Catalysis, Vol. 105; Elsevier: Amsterdam, 1997; pp 795−800.
(17) Gonthier, S.; Thompson, R. W. In *Advanced Zeolite Science and Applications;* Jansen, J. C., Stocker, M., Karge, H. G., Weitkamp, J., Eds.; Studies in Surface Science and Catalysis, Vol. 85; Elsevier: Amsterdam, 1994; Chapter 2, p 43.
(18) Mertens, M.; Martens, J. A.; Grobet, P. J.; Jacobs, P. A. In *Guidelines for Mastering the Properties of Molecular Sieves. Relationship between the Physicochemical Properties of Zeolitic Systems and Their Low Dimensionality*; Barthomeuf, D., Derouane, E. G., Hölderich, W., Eds.; NATO ASI Series B 221; Plenum: New York, 1990; p 1.
(19) Hartmann, M.; Azuma, N.; Kevan, L. *J. Phys. Chem.* **1995**, *99*, 10988.
(20) Ashtekar, S.; Chilukuri, S. V. V.; Prakash, A. M.; Harendranath, C. S.; Chakrabarty, D. K. *J. Phys. Chem.* **1995**, *99*, 6937.

(21) Ashtekar, S.; Chilukuri, S. V. V.; Prakash, A. M.; Chakrabarty, D. K. *J. Phys. Chem.* **1996**, *100*, 3665.

(22) Blackwell, C. S.; Patton, R. L. *J. Phys. Chem.* **1984**, *88*, 6135.

(23) Goepper, M.; Guth, F.; Delmotte, L.; Guth, J. L.; Kessler, H. In *Zeolites: Facts, Figures, Future*; Jacobs, P. A., van Santen, R. A., Eds.; Studies in Surface Science and Catalysis, Vol. 49; Elsevier: Amsterdam, 1989; pp 857−866.

(24) Maistriau, L.; Gabelica, Z.; Derouane, E. G.; Vogt, E. T. C.; van Oene, J. *Zeolites* **1991**, *11*, 583.

(25) Makinen, M. W.; Kuo, L. C.; Yim, M. B.; Wells, G. B.; Fukuyama, J. M.; Kim, J. E. *J. Am. Chem. Soc.* **1985**, *107*, 5245.

(26) Iton, L. E.; Choi, I.; Desjardins, J. A.; Maroni, V. A. *Zeolites* **1989**, *9*, 535.

(27) Mizuno, K.; Imamura, S.; Lunsford, J. H. *Inorg. Chem.* **1984**, *23*, 3510.

(28) Nishida, Y.; Kida, S. *Bull. Chem. Soc. Jpn.* **1975**, *48*, 1045.

(29) Nishida, Y.; Shimohori, H. *Bull. Chem. Soc. Jpn.* **1973**, *46*, 2406.

(30) Bencini, A.; Gatteschi, D. In *Transition Metal Chemistry*; Melson, G. A., Figgis, B. N., Eds.; Marcel Dekker: New York, 1982; Vol. 8, Chapter 1, pp 1−78.

(31) De Vos, D. E.; Feijen, E. J. P.; Schoonheydt, R. A.; Jacobs, P. A. *J. Am. Chem. Soc.* **1994**, *116*, 4746.

(32) Brouet, G.; Chen, X.; Lee, C. W.; Kevan, L. *J. Am. Chem. Soc.* **1992**, *114*, 3720.

(33) Azuma, N.; Lee, C. W.; Zamadics, M.; Kevan, L. In *Zeolites and Related Microporous Materials: State of the Art 1994*; Weitkamp, J., Karge, H. G., Pfeifer, H., Holderich, W., Eds.; Studies in Surface Science and Catalysis, Vol. 84; Elsevier: Amsterdam, 1994; pp 805−812.

(34) Marchese, L.; Martra, G.; Damilano, N.; Coluccia, S.; Thomas, J. M. In *11th International Congress on Catalysis-40th Anniversary*; Hightower, J. W., Delgass, W. N., Iglesia, E., Bell, A. T., Eds.; Studies in Surface Science and Catalysis, Vol. 101; Elsevier: Amsterdam, 1996; pp 861−870.